Research Journal of Applied Sciences, Engineering and Technology 6(19): 3495-3505, 2013
DOI:10.19026/rjaset.6.3552
ISSN: 2040-7459; e-ISSN: 2040-7467

Submitted: August 15, 2012 Accepted: September 12, 2012 Published: October 20, 2013

Research Article

Buckling and Free Vibrations of Cylindrical Stiffened Composite Shells with Internal Liquid

J.E. Jam and M.A. Nikjoo
Composite Materials and Technology Center, MUT, Tehran, Iran

Abstract: The free vibration and buckling of cylindrical composite shell with internal liquid is studied in this study. The shell composed of several composite layers and stiffeners which are rings and stringers. The first order shear theory was used for shell and stiffeners. Stiffeners were used in equations as discrete elements. The effects of axial force, internal pressure and shell rotation about cylinder axis, were calculated. The Reily-Ritz method was used for solving the problem. The potential and kinetic energy of shell and each stiffeners and kinetic energy of liquid are substituted in the functional of energy. The natural frequencies and the critical axial forces in each mode is obtained. The section shape of each stiffener is rectangle. The stringers can have variable height in their length (a parabolic shape for example) and its effect is studied for shell with and without liquid. Also Stiffened composite shell with different internal pressure, different axial forces and different rotation speeds is studied. The liquid is ideal and sloshing was neglected.

Keywords: Buckling, cylindrical shell, ring, stiffener, stringer

INTRODUCTION

Dynamics of thin-walled cylindrical shells has been widely studied in recent decades. In the past years, these studies have been based on the classic theory of shells. Many of the engineering applications, including petrochemical industries, chemical process equipments, energy production devices, water transmission lines and etc. need tanks and pipes for storage and transportation of fluids, hence hereby the importance of studying the rotary or fixed cylindrical tanks and shells is stressed for these applications.

In the past, the classical theory of plates and shells was used, but by the introduction and application of composite materials in industrial scales, it was perceived that the application of classical theory for plates and shells composed of composite materials might be accompanied by very erroneous results. The above stated problems made the researchers use the first order and other higher order theories. In this research, the first order theory has been used. In comparison to the classic theory and higher order theories, the first order shear theory is a combination of more accuracy with respect to the classic theory and also needs less computation than higher order theories.

One of the other problems considered these days, is achievement of the best vibration and buckling state in shells, i.e., finding the optimum state for a certain desired design. Hence, different optimization methods were developed, wherein the genetic algorithm was a simple, but effective method and considerable attention is paid to it in terms of optimization, thanks to the speed of advanced computers now commercially available.

Zhi *et al*. (2008) have investigated the free vibrations of a cylindrical shell reinforced with rings, under arbitrary boundary conditions. Jafari and Bagheri (2006) studied the free vibrations of a thin cylindrical shell reinforced with rings, in which the distances between the rings and also their offsets were variable. In the same year, Rong-Tyai and Zung-Xian (2006) studied the vibrations of a composite cylindrical shell reinforced with rings, wherein the rings were homogenous and the distances were equal, but the first order shear theory was used then. Ramezani and Ahmadian (2009) studied all boundary conditions in free vibration of rotary cylindrical shell with combining the layer wise and wave propagation methods.

Bagheri and Jafari (2011) studied the free vibrations of a cylindrical shell reinforced with rings, having unequal distances and offsets; in order to reach the best optimized vibration state. Amabili (1997) studied the vibrations of a vessel with internal non-viscous incompressible fluid, where the effects of vibrations of the free surface of the fluid and the hydrostatic pressure were ignored and Reily-Ritz method was used to calculate the mode shapes.

In this study, buckling and free vibration of a stiffened cylindrical composite shell with and without liquid and with different rotation speed, internal pressure and axial load is investigated.

Corresponding Author: J.E. Jam, Composite Materials and Technology Center, MUT, Tehran, Iran

MATERIALS AND METHODS

Shell energy: Displacement equations of a composite cylindrical shell have been derived, using the first order shear theory. In this theory, the displacement of the middle surface of the shell is taken as reference and the displacements of the other points are related to the middle surface as follows:

$$u = u_0(x,\theta) + z\psi_x(x,\theta),$$
$$v = v_0(x,\theta) + z\psi_\theta(x,\theta), \quad (1)$$
$$w = w_0(x,\theta)$$

We can see displacement variables in Fig. 1. In relation 1, u_0, v_0 and w_0 are displacements of the middle surface along the x, θ and z directions, respectively. ψ_x and ψ_θ are the rotations of the middle surface around x and θ directions. Also, z is the distance of each point of the shell from the middle surface.

Using the equations of displacement-strain in cylindrical coordinate system and ignoring the second order terms, the following relations are achieved, wherein R is the radius of the middle surface of the shell:

$$\varepsilon_x = \frac{\partial u}{\partial x},\ \varepsilon_\theta = \frac{1}{R}\left(\frac{\partial v}{\partial x} + w\right),$$
$$\varepsilon_z = \frac{\partial w}{\partial z},\ \gamma_{\theta z} = \frac{\partial v}{\partial z} + \frac{1}{R}\left(\frac{\partial w}{\partial \theta}\right) - \frac{v_0}{R},$$
$$\gamma_{\theta z} = \frac{\partial u}{\partial z} + \frac{\partial w}{\partial x},\ \gamma_{x\theta} = \frac{1}{R}\frac{\partial u}{\partial \theta} + \frac{\partial v}{\partial x} \quad (2)$$

Also, based on the thickness variable, the strains can be stated:

$$\{\varepsilon\} = \{\varepsilon^{0*}\} + z\{\varepsilon^1\} \quad (3)$$

Strain vector is considered as:

$$\varepsilon^T = \{\varepsilon_x^0 \quad \varepsilon_\theta^0 \quad \gamma_{x\theta}^0 \quad k_x \quad k_\theta \quad k_{x\theta} \quad \gamma_{\theta z}^0 \quad \gamma_{xz}^0\} \quad (4)$$

In the above relations, $\boldsymbol{\varepsilon_x^0}$ and $\boldsymbol{\varepsilon_\theta^0}$ are the strains of the mid-surface, k_x, k_θ and $k_{x\theta}$ are the curvedness of mid-surface and $\gamma_{\theta z}^0$ and γ_{xz}^0 are the transverse shear values. By substituting relation 1 in relations 2, the strain matrix components can be achieved as following:

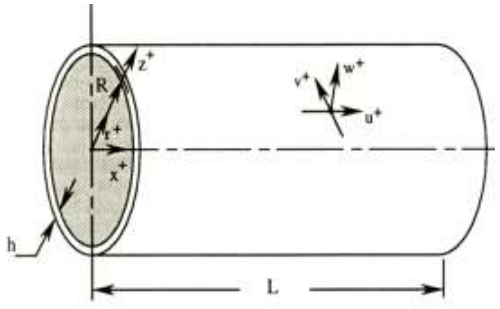

Fig. 1: A schematic of the cylindrical shell and displacement variables

$$\varepsilon_x^0 = \frac{\partial u_0}{\partial x},\ \varepsilon_\theta^0 = \frac{1}{R}\left(\frac{\partial v_0}{\partial \theta} + w_0\right),$$
$$\gamma_{x\theta}^0 = \frac{1}{R}\left(\frac{\partial u_0}{\partial \theta}\right) + \frac{\partial v_0}{\partial x},\ k_x = \frac{\partial \psi_x}{\partial x},$$
$$k_\theta = \frac{1}{R}\left(\frac{\partial \psi_\theta}{\partial \theta}\right),\ k_{x\theta} = \frac{1}{R}\left(\frac{\partial \psi_x}{\partial \theta}\right) + \frac{\partial \psi_\theta}{\partial x},$$
$$\gamma_{xz}^0 = \psi_x + \frac{\partial w_0}{\partial x},\ \gamma_{\theta z}^0 = \psi_\theta + \frac{\partial w_0}{R\partial \theta} - \frac{v_0}{R} \quad (5)$$

Generally, the stiffness matrix for an orthotropic material is:

$$[S] = \begin{bmatrix} A_{11} & A_{12} & A_{16} & B_{11} & B_{12} & B_{16} & 0 & 0 \\ A_{12} & A_{22} & A_{26} & B_{12} & B_{22} & B_{26} & 0 & 0 \\ A_{16} & A_{26} & A_{66} & B_{16} & B_{26} & B_{66} & 0 & 0 \\ B_{11} & B_{12} & B_{16} & D_{11} & D_{12} & D_{16} & 0 & 0 \\ B_{12} & B_{22} & B_{26} & D_{12} & D_{22} & D_{26} & 0 & 0 \\ B_{16} & B_{26} & B_{66} & D_{16} & D_{26} & D_{66} & 0 & 0 \\ 0 & 0 & 0 & 0 & 0 & 0 & H_{44} & H_{45} \\ 0 & 0 & 0 & 0 & 0 & 0 & H_{45} & H_{55} \end{bmatrix} \quad (6)$$

Wherein, the components are:

$$A_{ij} = \sum_{k=1}^{N}\left(\overline{Q_{ij}}\right)_k (z_k - z_{k-1}),$$
$$B_{ij} = \frac{1}{2}\sum_{k=1}^{N}\left(\overline{Q_{ij}}\right)_k (z_k^2 - z_{k-1}^2),$$
$$D_{ij} = \frac{1}{3}\sum_{k=1}^{N}\left(\overline{Q_{ij}}\right)_k (z_k^3 - z_{k-1}^3),$$
$$H_{ij} = k_0\sum_{k=1}^{N}\left(\overline{Q_{ij}}\right)_k (z_k - z_{k+1}), \quad (7)$$

where, z_k and z_{k-1} show the distances of the middle surface from the outer and inner surfaces of the k-th layer, as indicated in Fig. 2. N indicates the number of

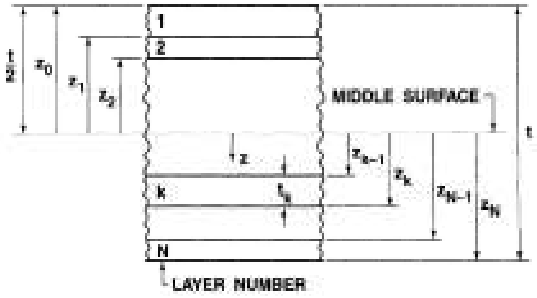

Fig. 2: Number of layers and their distance from the mid-surface

layers and $\overline{Q_{ij}}$ is the transformed stiffness matrix for the k-th layer. Also, k_0 is the shear correction factor. $\overline{Q_{ij}}$ is defined as:

$$\left[\overline{Q}\right] = [T]^{-1}[Q][T]^{-T} \tag{8}$$

where,

Q = The reduced stiffness matrix for the orthotropic material

T = The rotation matrix

Eventually, the potential energy of the shell is calculated from the following relation:

$$U_{shell} = \frac{1}{2}\int_0^l \int_0^{2\pi} \varepsilon^T [S] \varepsilon R\, d\theta\, dx \tag{9}$$

where,

l = The length of the cylinder

ε = The strain vector

S = The stiffness matrix

Potential strain energy due to rotation is:

$$U_{h,e} = \frac{h}{2}\int_0^L \int_0^{2\pi} N_{\theta e} \begin{Bmatrix} \left[\frac{1}{R}\frac{\partial u}{\partial \theta}\right]^2 + \\ \left[\frac{1}{R}\left(w + \frac{\partial v}{\partial \theta}\right)\right]^2 + \\ \left[\frac{1}{R}\left(v - \frac{\partial w}{\partial \theta}\right)\right]^2 \end{Bmatrix} R d\theta dx \tag{10}$$

where $N_{\theta,e}$ is:

$$N_{\theta,e} = \rho R^2 \Omega^2 \tag{11}$$

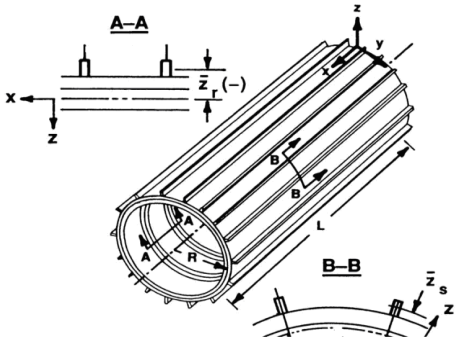

Fig. 3: Cylindrical reinforced shell

Potential energy due to axial force (N_a):

$$U_{Na} = -N_a \int_0^L \int_0^{2\pi} \begin{bmatrix} \left(\frac{\partial u}{\partial x}\right)^2 + \\ \left(\frac{\partial v}{\partial x}\right)^2 + \\ \left(\frac{\partial w}{\partial x}\right)^2 \end{bmatrix} R\, d\theta dx \tag{12}$$

Kinematic energy of the shell is also found by:

$$T = \frac{1}{2}\rho h \int_0^L \int_0^{2\pi} \begin{bmatrix} \dot{u}^2 + \dot{v}^2 + \dot{w}^2 + \\ 2\Omega(v\dot{w} - w\dot{v}) + \\ \Omega^2(v^2 + w^2) \end{bmatrix} R\, d\theta dx \tag{13}$$

The potential energies of inside pressure given by:

$$U_P = \int_0^L \int_0^{2\pi} \frac{P}{2}\left\{\left[\frac{\partial^2 w}{\partial \theta^2} + w\right] w\right\} d\theta dx + \frac{P}{4}\int_0^L \int_0^{2\pi} \left(\frac{\partial w}{\partial x}\right)^2 R^2 d\theta dx \tag{14}$$

where P is internal pressure.

Calculation of the energy of stiffeners: In Fig. 3, the cylindrical reinforced shell is shown. The offset of stiffeners, which is the distance of the middle surface of the shell from the middle surface of the stiffener, have been shown by $\overline{Z_s}$ and $\overline{Z_r}$, which indicate stringer and ring, respectively. The stiffeners used in the present research are all of rectangular cross-section and their height and thickness are shown by d and b, respectively (Fig. 4). These values with the subscript of r indicate rings and with the subscript of s indicate stringers.

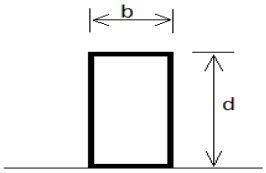

Fig. 4: A section of the stiffeners

Energy of the rings: First, the following are defined:

$$I_{zri} = \frac{b_{ri} d_{ri}^3}{12},$$
$$I_{xri} = \frac{b_{ri}^3 d_{ri}}{12},\ A_{ri} = b_{ri} d_{ri},\ \bar{z}_{ri} = \pm\frac{h + d_{ri}}{2},$$
$$J_{ri} = \frac{1}{3}\left[1 - \frac{192 b_{ri}}{\pi^5 d_{ri}} \sum_{n=1,3,5,\ldots}^{\infty} \frac{1}{n^5} \tanh\left(\frac{n\pi d_{ri}}{2 b_{ri}}\right)\right] b_{ri}^3 d_{ri} \tag{15}$$

In relation 12, the index *ri* indicates the *i*-th ring. I_{xri}, l_{zri} are the second moments of the ring cross-section around axes, passing through the center of the ring cross-section, respectively, which are parallel with the x and z axes. A_{ri} is the area of the cross-section and J_{ri} is the flexural stiffness of the ring. Eventually, $\overline{Z_{ri}}$ is the offset of the ring, whose value is positive for the external ring and negative for the internal ring. The potential energy of the ring is achieved from the following relation:

$$U_{ri} = \int_0^{2\pi} \left\{ \begin{array}{l} \frac{E_{ri} I_{zri}}{2} \frac{1}{\left(R + \bar{z}_{ri}\right)} \left[\frac{\partial w_{ri}}{\partial x} + \frac{1}{\left(R + \bar{z}_{ri}\right)} \frac{\partial^2 u_{ri}}{\partial \theta^2}\right]^2 + \\ \frac{E_{ri} I_{xri}}{2} \frac{1}{\left(R + \bar{z}_{ri}\right)^3} \left[w_{ri} + \frac{\partial^2 w_{ri}}{\partial \theta^2}\right]^2 + \\ \frac{E_{ri} A_{ri}}{2} \frac{1}{\left(R + \bar{z}_{ri}\right)} \left[\frac{\partial v_{ri}}{\partial \theta} - w_{ri}\right]^2 + \\ \frac{G_{ri} J_{ri}}{2} \frac{1}{\left(R + \bar{z}_{ri}\right)} \left[\frac{\partial^2 w_{ri}}{\partial x \partial \theta} + \frac{1}{\left(R + \bar{z}_{ri}\right)} \frac{\partial u_{ri}}{\partial \theta}\right]^2 \end{array} \right\} d\theta \tag{16}$$

where in:

$$u_{ri} = u_0 + \overline{z_{ri}} \psi_x,$$
$$v_{ri} = v_0 \left(1 + \frac{\overline{z_{ri}}}{R}\right) + \overline{z_{ri}} \psi_\theta,\ w_{ri} = w_0 \tag{17}$$

The kinetic energy of the ring is calculated as follows:

$$T_{ri} = \frac{\rho_{ri}}{2} \int_0^{2\pi} \left\{ \begin{array}{l} A_{ri}\left[\dot{u}_{ri}^2 + \dot{v}_{ri}^2 + \dot{w}_{ri}^2 + \right] + \\ 2\Omega(v_{ri} \dot{w}_{ri} - \dot{v}_{ri} w_{ri}) + \\ \Omega^2 (v_{ri}^2 + w_{ri}^2) + \\ J_{ri}\left(\dot{\psi}_x\right)^2 + I_{xri}\left(\dot{\psi}_\theta\right)^2 \end{array} \right\} \left(R + \bar{z}_{ri}\right) d\theta \tag{18}$$

Potential energy of the rings due to rotation:

$$U_{h,r} = \frac{1}{2} \sum_{k=1}^{Nr} \int_0^{2\pi} N_{\theta,r} \left\{ \begin{array}{l} \left[\frac{1}{R} \frac{\partial u_r}{\partial \theta}\right]^2 + \\ \left[\frac{1}{R}\left(w_r + \frac{\partial v_r}{\partial \theta}\right)\right]^2 + \\ \left[\frac{1}{R}\left(v_r - \frac{\partial w_r}{\partial \theta}\right)\right]^2 \end{array} \right\} R d\theta \tag{19}$$

where $N_{\theta,r}$ is:

$$N_{\theta,r} = \rho_r R^2 \Omega^2 \tag{20}$$

where ρ_r is the density of K-th ring.

Energy of the stringers: First, the following must be defined:

$$I_{ysi}(x) = \frac{b_{si} d_{si}^3(x)}{12},\ I_{zsi}(x) = \frac{b_{si}^3 d_{si}(x)}{12},$$
$$A_{sj}(x) = b_{sj} d_{sj}(x),\ \bar{z}_{sj}(x) = \pm\frac{h + d_{sj}(x)}{2}, \tag{21}$$
$$J_{sj}(x) = \frac{1}{3}\left[1 - \frac{192 b_{sj}}{\pi^5 d_{sj}(x)} \times \sum_{n=1,3,5,\ldots}^{\infty} \frac{1}{n^5} \tanh\left(\frac{n\pi d_{sj}(x)}{2 b_{sj}}\right)\right] b_{sj}^3 d_{sj}(x)$$

In relations 16, the index *sj* indicates the *j*-th stringer. I_{ysj}, l_{zsj} are the second moments of the cross-section around the two axes perpendicular to each other, respectively. $A_{sj}(x)$ is the area of the cross-section and $J_{sj}(x)$ is the flexural stiffness of the stringer. Eventually, $\bar{z}_{sj}(x)$ is the offset of the stringer, whose value is positive for the external stringer and negative for the internal stringer.

The potential strain energy of the stringer is achieved as follows:

$$U_{sj} = \frac{E_{sj}}{2}\int_0^l \left\{ \begin{array}{l} I_{ysj}\left[\frac{\partial^2 w_{sj}}{\partial x^2}\right]^2 + \\ I_{zsj}\left[\frac{\partial^2 v_{sj}}{\partial x^2}\right]^2 + \\ A_{sj}\left[\frac{\partial u_{sj}}{\partial x}\right]^2 \end{array} \right\} dx + \int_0^l \frac{G_{sj}J_{ysj}}{2R^2}\left[\frac{\partial^2 w_{sj}}{\partial x\,\partial\theta}\right]^2 dx \quad (22)$$

In which:

$$\begin{aligned} u_{sj} &= u_0 + \overline{z_{sj}}\psi_x, \\ v_{sj} &= v_0\left(1 + \frac{\overline{z_{sj}}}{R}\right) + \overline{z_{sj}}\psi_\theta, \\ w_{sj} &= w_0 \end{aligned} \quad (23)$$

Potential energy of stringers due to axial force (N_a):

$$U_{Na,s} = -N_a\sum_{k=1}^{Ns}\int_0^l \left[\begin{array}{l} \left(\frac{\partial u_s}{\partial x}\right)^2 + \\ \left(\frac{\partial v_s}{\partial x}\right)^2 + \\ \left(\frac{\partial w_s}{\partial x}\right)^2 \end{array}\right] dx \quad (24)$$

The kinetic energy of the stringer is achieved as follows:

$$T_{sj} = \frac{\rho_{sj}}{2}\int_0^l \left\{ \begin{array}{l} A_{sj}\left[\dot{u}_{sj}^2 + \dot{v}_{sj}^2 + \dot{w}_{sj}^2\right] + \\ 2\Omega(v_{sj}\dot{w}_{sj} - \dot{v}_{sj}w_{sj}) + \\ \Omega^2(v_{sj}^2 + w_{sj}^2) + \\ J_{sj}\left(\dot{\psi}_\theta\right)^2 + I_{xsj}\left(\dot{\psi}_x\right)^2 \end{array} \right\} dx \quad (25)$$

Investigation of the effect of internal fluid on vibrations of cylindrical shell: In order to investigate the effect of internal fluid on vibrations of the cylindrical shell, one should analyze the interaction between the solid and fluid states at their interface, using a mathematical model. Assumptions of the mathematical model are as follows:

- Flow of the fluid is a potential flow.
- Fluid is ideal, i.e. is non-viscous and incompressible.
- Displacements are small, so that the linear theory can be used.
- Velocity of the fluid along the cylinder axis is zero.
- Effects of the surface waves are ignored.

Regarding the first assumption of potential flow, the potential flow function in the cylindrical coordinate system can be written as:

$$\begin{aligned} &\nabla^2\Phi = 0 \\ &\frac{\partial^2\Phi}{\partial r^2} + \frac{1}{r}\frac{\partial\Phi}{\partial r} + \frac{1}{r^2}\frac{\partial^2\Phi}{\partial\theta^2} + \frac{\partial^2\Phi}{\partial x^2} = 0 \end{aligned} \quad (26)$$

Where in, Φ is the velocity potential function of the fluid and x, θ and r are axial, circumferential and radial components in the cylindrical coordinate system, respectively.

Components of the velocity of fluid flow are determined as follows:

$$\begin{aligned} V_x &= \frac{\partial\Phi}{\partial x} \\ V_\theta &= \frac{1}{R}\frac{\partial\Phi}{\partial\theta} \\ V_r &= \frac{\partial\Phi}{\partial r} \end{aligned} \quad (27)$$

V_r, V_θ, V_x are components of fluid velocity along the axial, circumferential and radial directions, respectively. In order to find the effects of the fluid, one should consider the boundary conditions caused by the interaction between fluid and solid and apply them in the differential equations of the fluid. Hence, regarding the fact that the fluid does not penetrate into the shell, there is always a constant touch between the outer fluid layer and the internal wall of the shell and the radial velocity component of the fluid is the same constant as that of the shell at their interface. These assumptions can be defined through the following equation:

$$V_{r|r=R} = \frac{\partial\Phi}{\partial r}\Big|_{r=R} = \left(\frac{\partial w}{\partial t}\right)_{r=R} \quad (28)$$

In order to solve the differential equation of the velocity potential function, the method of separation of

the variables can be used. Therefore, the velocity potential is considered as the product of the two functions, as below:

$$\Phi(x,\theta,r,t) = R(r)S(x,\theta,t) \tag{29}$$

So as to solve find the $S(x,\theta,t)$ function, one can apply the boundary conditions of relation 28. By application of boundary conditions and substituting the above relation into the boundary condition relation, Eq. (30) will be achieved:

$$\Phi(x,\theta,r,t) = \frac{R(r)}{\left(\frac{\partial R(r)}{\partial r}\right)_{r=R}} \frac{\partial w(x,\theta,t)}{\partial t} \tag{30}$$

where, w is the displacement of the shell in its radial direction.

Substituting relation 30 in the flow potential function (relation 26) and performing the mathematical simplifications, the homogenous Bessel function is resulted as follows:

$$r^2 \frac{d^2R(r)}{dr^2} + r\frac{dR(r)}{dr} + R(r)[i^2k_r^2r^2 - n^2] = 0 \tag{31}$$

Where in, k_r is the number of radial half waves, i.e.:

$$k_r^2 = \left(\frac{m\pi}{l}\right)^2 - \left(\frac{\omega}{c_f}\right)^2 \tag{32}$$

For a shell exposed to an internal fluid, the factor of *R(r)* is always negative in relation 31; therefore, the general answer of Eq. (31) is expressed as:

$$R(r) = AJ_n(ik_r r) + BY_n(ik_r r) \tag{33}$$

where, J_n is the type one Bessel function and Y_n is Bessel function of *n*- order and r is the radial component in cylindrical coordinate system. For a cylinder filled up with fluid, the constant B must be set to zero, because the function is singular at the center of the cylinder (r = 0).

Kinetic energy of the fluid which is resulted from the movement of the internal fluid due to the shell displacement is derived as follows:

$$T_{fl} = \frac{1}{2}\rho_{fl}\int_0^R\int_0^{2\pi}\int_0^l rv^2 dx\, d\theta\, dr \tag{34}$$

Where, v is velocity and P_{fl} is the fluid density.

The square of fluid velocity is equal to the sum of the squares of the velocity components in the axial, circumferential and radial directions, as follows:

$$v^2 = v_x^2 + v_\theta^2 + v_r^2 \tag{35}$$

By considering the fluid as incompressible and neglecting the effects of surface waves, the potential energy of the fluid is equal to zero.

The following functions are adopted to separate the spatial variable *x, θ* and the time variable *t*:

$$\begin{aligned}
u_0(x,\theta,t) &= A\cos\left(\frac{m\pi x}{l}\right)\cos(n\theta)e^{i\omega t}\\
v_0(x,\theta,t) &= B\sin\left(\frac{m\pi x}{l}\right)\sin(n\theta)e^{i\omega t}\\
w_0(x,\theta,t) &= C\sin\left(\frac{m\pi x}{l}\right)\cos(n\theta)e^{i\omega t}\\
\psi_x(x,\theta,t) &= D\cos\left(\frac{m\pi x}{l}\right)\cos(n\theta)e^{i\omega t}\\
\psi_\theta(x,\theta,t) &= E\sin\left(\frac{m\pi x}{l}\right)\sin(n\theta)e^{i\omega t}
\end{aligned} \tag{36}$$

Formation of the potential energy function: Now, having the potential and kinetic energies of the shell, fluid and stiffeners, one can form the potential energy function as follows, where *n* is the number of rings and *m* is the number of stringers (Jafari and Bagheri, 2006):

$$\begin{aligned}
F = {} & T_{fl} - U_{shell} + T_{shell} + U_h + U_{Na} + U_P +\\
& \sum_{i=1}^{n}(T_{ri} - U_{ri} - U_{h,r}) +\\
& \sum_{j=1}^{m}(T_{sj} - U_{sj} - U_{Na,s})
\end{aligned} \tag{37}$$

where,

T_{fl} = The kinetic energy of the fluid
U_{shell} = The potential strain energy of the shell
U_h = The potential energy of the shell due to rotation
U_{Na} = Potential energy of shell due to axial force
U_P = The potential energy due to pressure
T_{shell} = The kinetic energy of the shell
T_{ri} = The kinetic energy of one ring
U_{ri} = The potential strain energy of one ring
$U_{h,r}$ = The potential energy of the ring due to rotation
T_{sj} = The kinetic energy of one stringer
U_{sj} = The potential strain energy of one stringer
$U_{Na,s}$ = The potential energy of the stringer due to axial force

Problem solving: Reily-Ritz method has been used to solve the problem. This method is based on the

minimum potential energy method. According to Reily-Ritz method, in order for the potential energy which is a function of *A*, *B*, *C*, *D* and *E* to be a minimum, the differentiation of the total energy with respect to the factors applied in the displacement field, must go zero. Therefore, a differentiation is taken from the total energy of the system with respect to the stated factors and is set to zero. Then, a 5 Eq. (5) unknown differential set of equations is arrived at, wherein the *A*, *B*, *C*, *D* and *E* are its unknowns.

By reordering the terms, the following matrix relation is achieved:

$$\left[\left[K\right]-\omega^2\left[M\right]\right]\begin{Bmatrix}A\\B\\C\\D\\E\end{Bmatrix}=0 \tag{38}$$

Where in, *K* and *M* are the stiffness and mass matrices of the structure, respectively. The components of the matrix *K* involve the geometrical dimensions and the physical specifications of the structure. In order to determine the non- evident answers of the relation (37), a generalized eigenvalue problem has to be solved. In order for the Eq. (37) to have a non- evident answer, the determinant of the factors must be set to zero:

$$\left|K-\omega^2 M\right|=0 \tag{39}$$

From the above, the natural frequencies for each of the (*m, n*) modes are achieved.

RESULTS AND DISCUSSION

Comparison of the results for the isotropic shell reinforced with ring and stringer: In Table 1 geometrical specifications of the shell and stiffeners is presented. In Table 2, the natural frequencies of the present research are compared with those of an experimental research and also those of an analytical research.

As it is seen in Table 2, there is a good convergence between the reference frequencies and the frequency achieved from the present research.

Table 1: Geometrical specifications of the shell and stiffeners

Characteristic	Size
Number of stringer/ring	13/20
Radius	0.203 m
Thickness	0.00204 m
Length	0.813 m
Height of stringer/ring	0.006/0.006 m
Width of stringer/ring	0.004/0.008 m
E	207 GPa
ν	0.3
ρ	7430 kg/m^3

Table 2: Comparison of the results of an isotropic shell reinforced with ring, and stringer without internal fluid

Present research	Mustafa and Ali (1989)	Experimental (ESDU, 1982)	n	m
929	942	938	1	1
430	439	443	2	1
334	337	348	3	1
485	482	492	4	1
739	740	745	5	1

Table 3: Geometrical specifications of the shell and fluid

Characteristic	Size
Radius	0.9
Radius to thickness ratio	60
Length to radius ratio	24.98
Density of the fluid	1000
Density of the shell	7812
E	203.4 GPa
ν	0.3

Table 4: Comparison of the results of isotropic shell with internal fluid

Present research	Toorani and Lakiss	Newredson	Lakiss and sino	m
4.268	4.1965	4.504	4.549	1
16.349	16.062	17.257	17.46	2
34.455	34.225	36.361	37.131	3
56.473	55.63	59.594	62.115	4

Table 5: Geometrical specifications of the shell and stiffeners

Characteristic	Size
Number of stringer	60
Radius	0.242 m
Thickness	0.00065 m
Length	0.6096 m
Height of stringer	0.00702 m
Width of stringer	0.00255 m
E	68.95 GPa
ν	0.3
ρ	2714 kg/m^3

Comparison of the results for the isotropic shell filled up with fluid: Specifications of the shell and fluid are included in Table 3:

In Table 4, natural frequencies of the present research are compared with a number of references. The unit of the frequencies is Hertz.

As it is realized, there is a good convergence between the reference frequencies and the frequency achieved from the present research.

Comparison of the results for the isotropic shell reinforced with stringer: Specifications of the shell and fluid are included in Table 5.

In Table 6, the natural frequencies of the present research are compared with those of an experimental research and also those of an analytical research.

As it is seen in Table 6, there is a good convergence between the reference frequencies and the frequency achieved from the present research.

Discussion: Here, natural frequencies of the system in different states are studied and the effective factors on

Table 6: Comparison of the results of an isotropic shell reinforced with stringer and without internal fluid

Present Research	Mustafa and Ali (1989)	Experimental (ESDU, 1982)	n	m
1135	1141		1	1
671	674		2	1
426	427		3	1
297	296		4	1
229	225	231	5	1
195	188	197	6	1
184	174	189	7	1
190	177	199	8	1
208	193	219	9	1

Table 7: Geometrical specifications of the shell

Characteristic	Size
L	1 m
R	0. 2 m
Thickness	0.002 m
Sequence of layers	(90, 0, 0, 90)

Table 8: Properties of the materials used in this section

Name of material	E11 (GPa)	E22 (GPa)	G12 (GPa)	ν	P (kg/m3)
Steel	206	206		0.3	7800
Carbon/Epoxy	139.4	8.35	3.1	0.27	1542

natural frequencies and buckling have been investigated. The specification of shell is seen in Table 7.

Characteristics of materials used in different sections of the investigation of the results, are presented in Table 8.

It is noteworthy that in all the investigated sections of the present project, the material of the stiffeners is steel and in the case of existence of fluid, water is the case. The boundary conditions of the shell are simply supported in two ends at all sections. The material of shell is carbon/epoxy and the "m" in mode shape is equal to 1.

Investigation of the effect of variable height of stringers on natural frequencies:

Shell has stringers with variable height and without internal liquid: The height of stringers varied in form of parabola that shown in Fig. 5.

Table 9 has 5 states for stringers. The state 1 and state 2 are parabola with maximum (Fig. 5, lower shape) and the state 4 and state 5 are parabola with minimum (Fig. 5, upper shape). The state 3 is a straight line.

Regarding the Fig. 6, in state 3 the natural base frequency is minimum.

In state 1 and state2 base frequencies are bigger than state3. The base frequency of state 1 that (d2/d1) is larger, is higher than state2.

In state 4 and state5 base frequencies are bigger than state3. The base frequency of state 5 that (d2/d1) is larger, is the highest frequency. Therefore with increasing the *d*2/*d*1 ratio, natural frequencies at base mode increase and the parabola with minimum for stringers has higher base frequency.

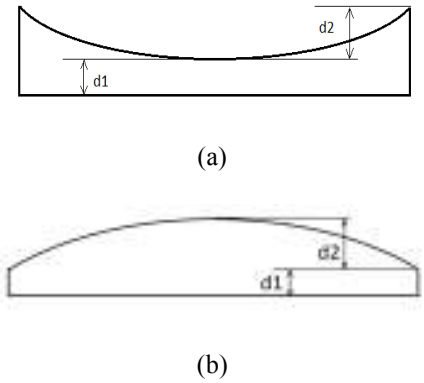

Fig. 5: Different height of stringers in parabolic form. Upper shape has minimum and lower shape has maximum

Table 9: The shapes of stringers

State number	Shape name	Distribution of height
1	Parabola with maximum	d1 = 15, d2 = 50
2	Parabola with maximum	d1 = 25, d2 = 30
3	Straight line	d1 = 40, d2 = 0
4	Parabola with minimum	d1 = 25, d2 = 30
5	Parabola with minimum	d1 = 15, d2 = 50

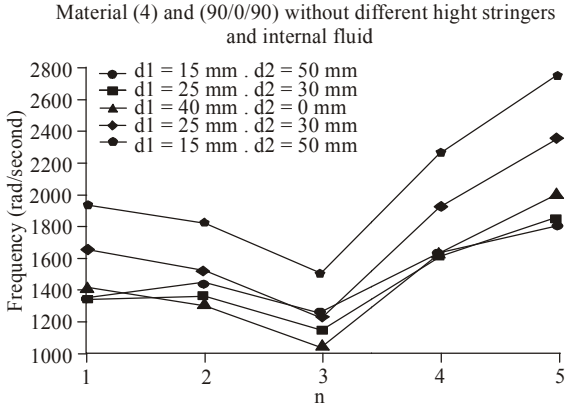

Fig. 6: The effect of stringer height on natural frequency of shell without liquid

Shell has stringers with variable height and with internal liquid: In this section the states is same as previous and the difference is the internal liquid.

Regarding the Fig. 7, in state 3 the natural frequency is minimum in all modes.

In state 1 and state2, base frequencies are bigger than states 3, 4 and 5. The base frequency of state 1 that (d2/d1) is larger, is the highest base frequency.

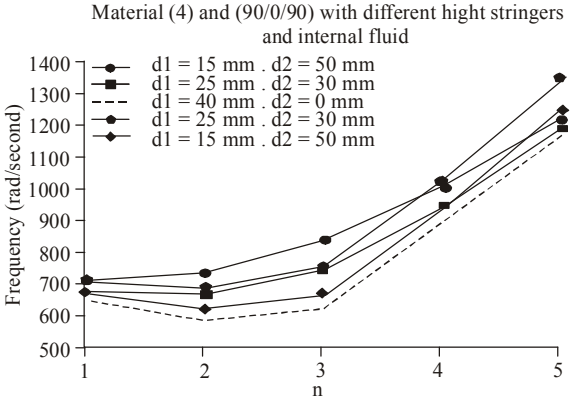

Fig. 7: The effect of stringer height on natural frequency of shell with liquid

Table 10: Geometrical specifications of the shell and stiffeners

Characteristic	Size
Height of stiffeners	0.01 m
Width of stiffeners	0. 002 m
Number of rings	5
Number of stringers	8
L	1 m
R	0. 2 m
Thickness	0.002 m
Sequence of layers	(90, 0, 0, 90)

ccIn state 4 and state5 base frequencies are bigger than state3. The base frequency of state 5 that (d2/d1) is larger, is higher than state 4. Therefore with increasing the *d*2/*d*1 ratio, natural frequencies at base mode increase and when we have internal liquid, the parabola with maximum for stringers has higher base frequency.

Investigation of the effect of rotation, axial force and pressure on buckling and natural frequencies: In this section the specification of shell is seen in Table 10:

Buckling of stiffened shell with different internal pressure: Regarding the Fig. 8, with increasing the internal pressure, critical buckling forces at different modes increase. In the pressure of -500 kPa, the shell collapsed in mode n = 3.

The differences between critical forces in each pressure in different modes are almost same. The minimum critical buckling forces in all speeds occur in mode m = 1 and n = 3.

Natural frequencies of stiffened shell with internal liquid and different internal pressure: Regarding the Fig. 9, with increasing the internal pressure, the natural frequencies in different modes and base frequency increase. In pressure of -500 kPa and in mode 3, because of shell collapsing natural frequency is zero. Internal pressure does not have any effects on mode n = 1and does not differing the natural frequency in this mode.

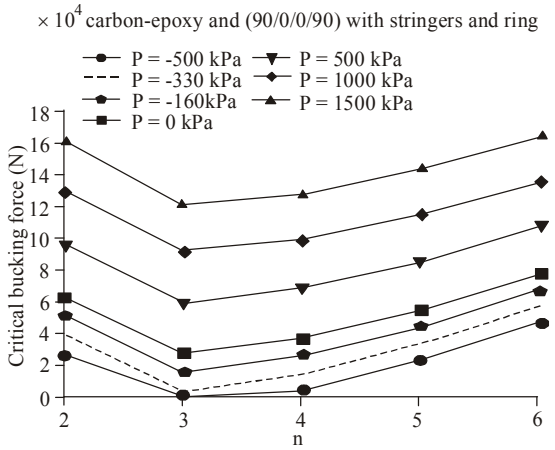

Fig. 8: Critical buckling forces of shell with different internal pressure

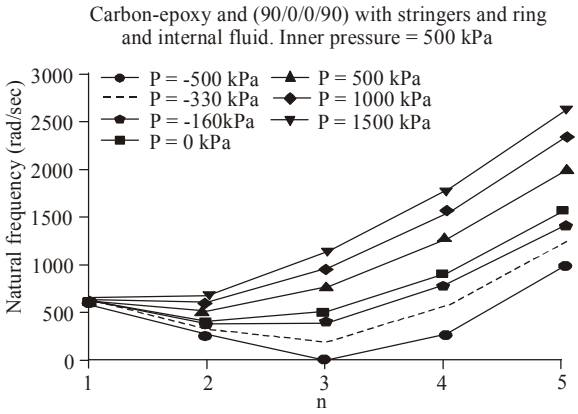

Fig. 9: Natural frequencies of stiffened composite cylindrical shell with internal liquid and different pressure

When pressure varying from -500 to 1500 kPa, mode switching occur two times. When pressure is -330 kPa and less, the base mode is m = 1 and n = 3. From -160 kPa to 1000 kPa, the base mode is m = 1 and n = 2. When the pressure is 1500 kPa and more, the base mode is m = 1 and n = 1.

If the purpose is increasing the base frequency with increasing internal pressure, increasing the pressure more than a certain pressure (1420 kPa in this case) can not increase the base frequency, because the base mode is n = 1 and the natural frequency in this mode dose not changing with internal pressure.

Buckling of rotary stiffened shell with internal pressure of 500 kPa: Regarding the Fig. 10, with increasing the speed of rotation, critical buckling forces at different modes increase. The differences between critical forces in each pressure in different modes are almost same.

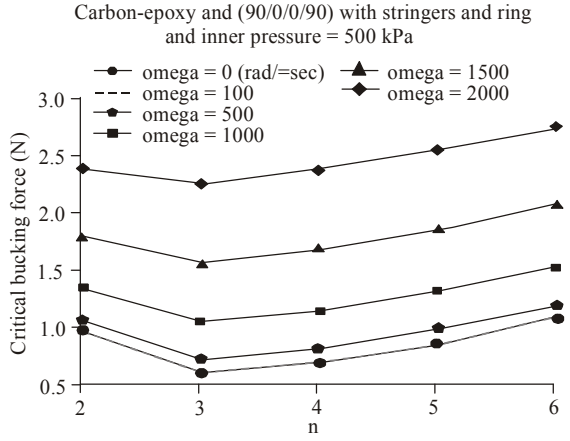

Fig. 10: Critical buckling forces of shell with different rotation speed

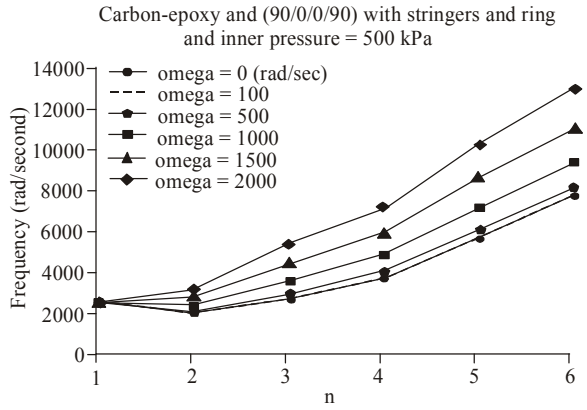

Fig. 11: Natural frequencies of shell with different rotation speeds

The minimum critical buckling forces in all speeds occur in mode m = 1 and n = 3.

Natural frequencies of rotary stiffened shell without internal liquid and with internal pressure of 500 kPa: Regarding the Fig. 11, with increasing the speed of rotation, natural frequencies at different modes increase. Speed of rotation does not have any effects on mode n = 1 and the natural frequency does not changing in this mode.

When rotation speed varying from 0 to 2000 rad/sec, mode switching occur one time. When the speed of rotation is 1000 rad/sec and less, the base mode is m = 1 and n = 2. When the speed of rotation is 1500 rad/sec and more, the base mode is m = 1 and n = 1.

When rotation speed varying from 0 to 2000 rad/sec, mode switching occur one time. When the speed of rotation is 1000 rad/sec and less, the base mode is m = 1 and n = 2. When the speed of rotation is 1500 rad/sec and more, the base mode is m = 1 and n = 1.

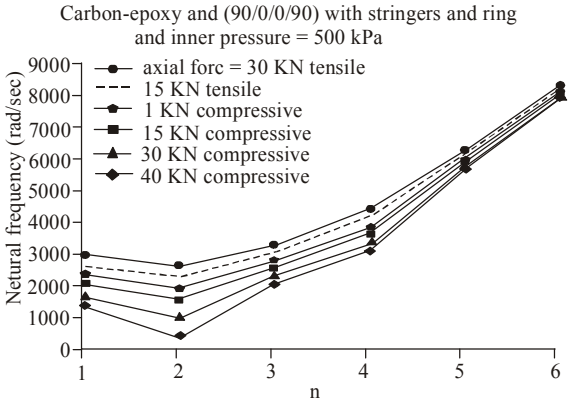

Fig. 12: Natural frequencies of shell with different axial loads

Natural frequencies of stiffened shell without internal liquid and with different axial loads: For all states in this section, the internal pressure is 500 kPa and the rotation speed is 500 rad/sec.

Regarding the Fig. 12, with increasing the compressive axial load, natural frequencies at different modes decrease and with increasing the tensile axial load, natural frequencies at different modes increase. In all states, the base frequencies occur in mode m = 1 and n = 2. Maximum difference is between base frequencies and with increasing n, the difference between natural frequency decrease.

CONCLUSION

- In stiffened composite shell without liquid, by increasing the *d*2/*d*1 ratio, natural frequencies at base mode increase and the parabola whit minimum for stringers has higher base frequency.
- In stiffened composite shell with internal liquid, by increasing the *d*2/*d*1 ratio, natural frequencies at base mode increase and the parabola with maximum for stringers has higher base frequency.
- In stiffened composite shell with increasing the internal pressure, critical buckling forces at different modes increase.
- In stiffened shell with internal liquid, by increasing the internal pressure, the natural frequencies in different modes and base frequency increase.
- In stiffened shell with internal liquid, with increasing the speed of rotation, critical buckling forces and natural frequencies at different modes increase.
- In stiffened shell with increasing the compressive axial load, natural frequencies decrease at different

modes and with increasing the tensile axial load, natural frequencies increase at different modes.

REFFERENCES

Amabili, M., 1997. Shell-plate interaction in the free vibration of circular cylindrical tanks partially filled with a liquid: The artificial spring method. J. Sound Vib., 199(3): 431-452.

Bagheri, M. and A.A. Jafari, 2011. Multi-objective optimization of ring stiffened cylindrical shells using a genetic algorithm. J. Sound Vib., 330(3): 374-384.

Jafari, A.A. and M. Bagheri, 2006. Free vibration of rotating ring stiffened cylindrical shells with non-uniform stiffener distribution. J. Sound Vib., 296 (1-2): 353-367.

Ramezani, S. and M.T. Ahmadian, 2009. Free vibration analysis of rotating laminated cylindrical shells under different boundary conditions using acombination of the layerwies theory and wave propagation approach. Trans. B Mech. Eng., 16(2): 168-176.

Rong-Tyai, W. and L. Zung-Xian, 2006. Vibration analysis of ring-stiffened cross-ply laminated cylindrical shells. J. Sound Vib., 295(3-5): 964-987.

Zhi, P., L. Xuebin and M. Janjun, 2008. A study on free vibration of a ring-stiffened thin circular cylindrical shell with arbitrary boundary conditions. J. Sound Vib., 314(1-2): 330-342.